AMERICAN SOCIETY FOR MICROBIOLOGY | Molecular and Cellular Biology®

RESEARCH ARTICLE

Astrocyte Elevated Gene 1 Interacts with Acetyltransferase p300 and c-Jun To Promote Tumor Aggressiveness

Liping Liu,[a,b] Hongyu Guan,[c] Yun Li,[d] Zhe Ying,[a,b] Jueheng Wu,[a] Xun Zhu,[a,b] Libing Song,[e] Jun Li,[a,f] Mengfeng Li[a,b]

Key Laboratory of Tropical Disease Control (Sun Yat-sen University), Chinese Ministry of Education, Guangzhou, Guangdong, China[a]; Department of Microbiology, Zhongshan School of Medicine,[b] Department of Endocrinology and Diabetes Center, The First Affiliated Hospital of Sun Yat-sen University,[c] Department of Experimental Research, Cancer Center,[e] and Department of Biochemistry, Zhongshan School of Medicine,[f] Sun Yat-sen University, Guangzhou, Guangdong, China; Department of Immunobiology, Jinan University, Guangzhou, Guangdong, China[d]

ABSTRACT Astrocyte elevated gene 1 (AEG-1) is an oncoprotein that strongly promotes the development and progression of cancers. However, the detailed underlying mechanisms through which AEG-1 enhances tumor development and progression remain to be determined. In this study, we identified c-Jun and p300 to be novel interacting partners of AEG-1 in gliomas. AEG-1 promoted c-Jun transcriptional activity by interacting with the c-Jun/p300 complex and inducing c-Jun acetylation. Furthermore, the AEG-1/c-Jun/p300 complex was found to bind the promoter of c-Jun downstream targeted genes, consequently establishing an acetylated chromatin state that favors transcriptional activation. Importantly, AEG-1/p300-mediated c-Jun acetylation resulted in the development of a more aggressive malignant phenotype in gliomas through a drastic increase in glioma cell proliferation and angiogenesis *in vitro* and *in vivo*. Consistently, the AEG-1 expression levels in clinical glioma specimens correlated with the status of c-Jun activation. Taken together, our results suggest that AEG-1 mediates a novel epigenetic mechanism that enhances c-Jun transcriptional activity to induce glioma progression and that AEG-1 might be a novel, potential target for the treatment of gliomas.

KEYWORDS E1A binding protein p300 (p300), acetylation, astrocyte elevated gene 1 (AEG-1), c-Jun transcription factor, glioma

Received 16 August 2016 **Returned for modification** 10 September 2016 **Accepted** 29 November 2016

Accepted manuscript posted online 12 December 2016

Citation Liu L, Guan H, Li Y, Ying Z, Wu J, Zhu X, Song L, Li J, Li M. 2017. Astrocyte elevated gene 1 interacts with acetyltransferase p300 and c-Jun to promote tumor aggressiveness. Mol Cell Biol 37:e00456-16. https://doi.org/10.1128/MCB.00456-16.

Address correspondence to Jun Li, lijun37@mail.sysu.edu.cn, or Mengfeng Li, limf@mail.sysu.edu.cn.

L.L. and H.G. contributed equally to this article.

Glioma is the most common and aggressive type of central nervous system tumor (1). Despite intensive research and clinical efforts, the prognosis for patients with this tumor type remains poor, largely attributable to its highly invasive and fast proliferating phenotype. The median life expectancy of patients with a grade IV glioma, known as a glioblastoma multiforme (GBM), is less than 1 year (2). Therefore, the definition of appropriate targets against which effective strategies to treat glioma may be developed represents a major goal in glioma research. A better comprehension of the molecular mechanisms mediating glioma progression is crucial to developing an efficacious therapeutic strategy that prevents the infiltration, invasion, and proliferation of glioma cells.

The product of the gene astrocyte elevated gene 1 (*AEG-1*), also known as the metadherin (*MTDH*) or *LYRIC* gene, was initially identified to be a novel protein whose expression is induced by human immunodeficiency virus type 1 (HIV-1) or by tumor necrosis factor alpha (TNF-α) in primary human fetal astrocytes (3–6). AEG-1 is a multifunctional protein that interacts with diverse partners in different types of cancers and promotes the development of essentially all hallmarks of cancer (7–12). Previous

studies have found that through its protein-protein interactions, the product of the *AEG-1* gene is a key pathological factor that regulates a variety of diseases associated with several signaling pathways, including the nuclear factor κB (NF-κB), phosphatidylinositol 3-kinase/AKT, mitogen-activated protein kinase (MAPK), and Wnt pathways (8, 13–17). Recently, Li et al. demonstrated that AEG-1 promotes gastric cancer progression through a positive-feedback Toll-like receptor 4/NF-κB signaling-related mechanism (14). Moreover, Robertson and colleagues found that AEG-1-deficient mice display resistance to *N*-nitrosodiethylamine-induced hepatocellular carcinoma and lung metastasis (18).

Although numerous studies have established a clinicopathological correlation between the levels of AEG-1 expression and various aspects of malignant features of cancer, the underlying molecular mechanism through which AEG-1 exerts its oncogenic activities requires further clarification. We previously demonstrated that AEG-1 upregulates matrix metallopeptidase 9 (MMP-9) expression, possibly through both NF-κB- and c-Jun-mediated mechanisms (19). In agreement with our results, Emdad et al. reported that AEG-1 interacts with p65 and promotes the nuclear translocation of NF-κB (7). However, the molecular mechanism through which AEG-1 activates the c-Jun pathway remains largely unknown.

In the current study, we identified AEG-1 to be a novel interacting partner of c-Jun and p300. Furthermore, we demonstrated that these interactions promote c-Jun acetylation and chromatin remodeling, which led to upregulated expression of the c-Jun target genes and, consequently, promoted angiogenesis and tumor cell survival. Our findings reveal a new molecular mechanism through which AEG-1 promotes cancer progression, which might further suggest a clinical value of AEG-1 as a novel therapeutic target.

RESULTS

AEG-1 enhances c-Jun transactivation in glioma cells. Our previous studies that indicated the essential involvement of AP-1 activation in the effects of AEG-1 on gliomagenesis (19) prompted us to further study the role of AEG-1 in c-Jun signaling. To this end, we first performed gene expression microarray analysis and found that the c-Jun target gene sets were downregulated in AEG-1-specific small interfering RNA (siRNA)-transfected cells compared with their regulation in scrambled siRNA-transfected control cells (Fig. 1A; see also Table S1 in the supplemental material). Next, we comparatively assessed the DNA-binding affinity of the c-Jun complex in AEG-1-overexpressing and AEG-1-knockdown glioma cell models (Fig. 1B) using an electrophoretic mobility shift assay (EMSA). As anticipated, the formation of the c-Jun/DNA complex was enhanced by ectopic expression of AEG-1 but was decreased by silencing of AEG-1 in glioma cells (Fig. 1C). Furthermore, the activity level of a luciferase reporter driven by the binding of the c-Jun-binding motif (TRE) was significantly increased in AEG-1-tranduced cells and was decreased in AEG-1-silenced cells (Fig. 1D). Taken together, these data suggest that AEG-1 promotes c-Jun transactivation and induces the expression of c-Jun-dependent downstream genes in glioma cells.

AEG-1 promotes the acetylation of c-Jun. Next, we explored the mechanism underlying AEG-1-mediated c-Jun transactivation. Because the increase in c-Jun activity is partially due to c-Jun phosphorylation, we began with examining the c-Jun phosphorylation levels in glioma cells subjected to AEG-1 overexpression or AEG-1 knockdown. Our results showed no significant change in the level of c-Jun phosphorylation upon AEG-1 overexpression or knockdown (Fig. 1E). As the transactivational activity of c-Jun is also modulated by c-Jun acetylation (20–22), we further sought to determine whether AEG-1 regulates c-Jun acetylation. As shown in Fig. 1F, the acetylation level of c-Jun was significantly increased in cells overexpressing AEG-1 and was significantly decreased in cells in which AEG-1 was knocked down compared with the AEG-1 levels in the control cells. Notably, the expression of a c-Jun mutant (K3R-c-Jun), which blocks acetylation-dependent AP-1 transactivation (20, 22), drastically diminished the stimulatory effect of AEG-1 on the transactivational activity of c-Jun (Fig. 1G), suggesting that

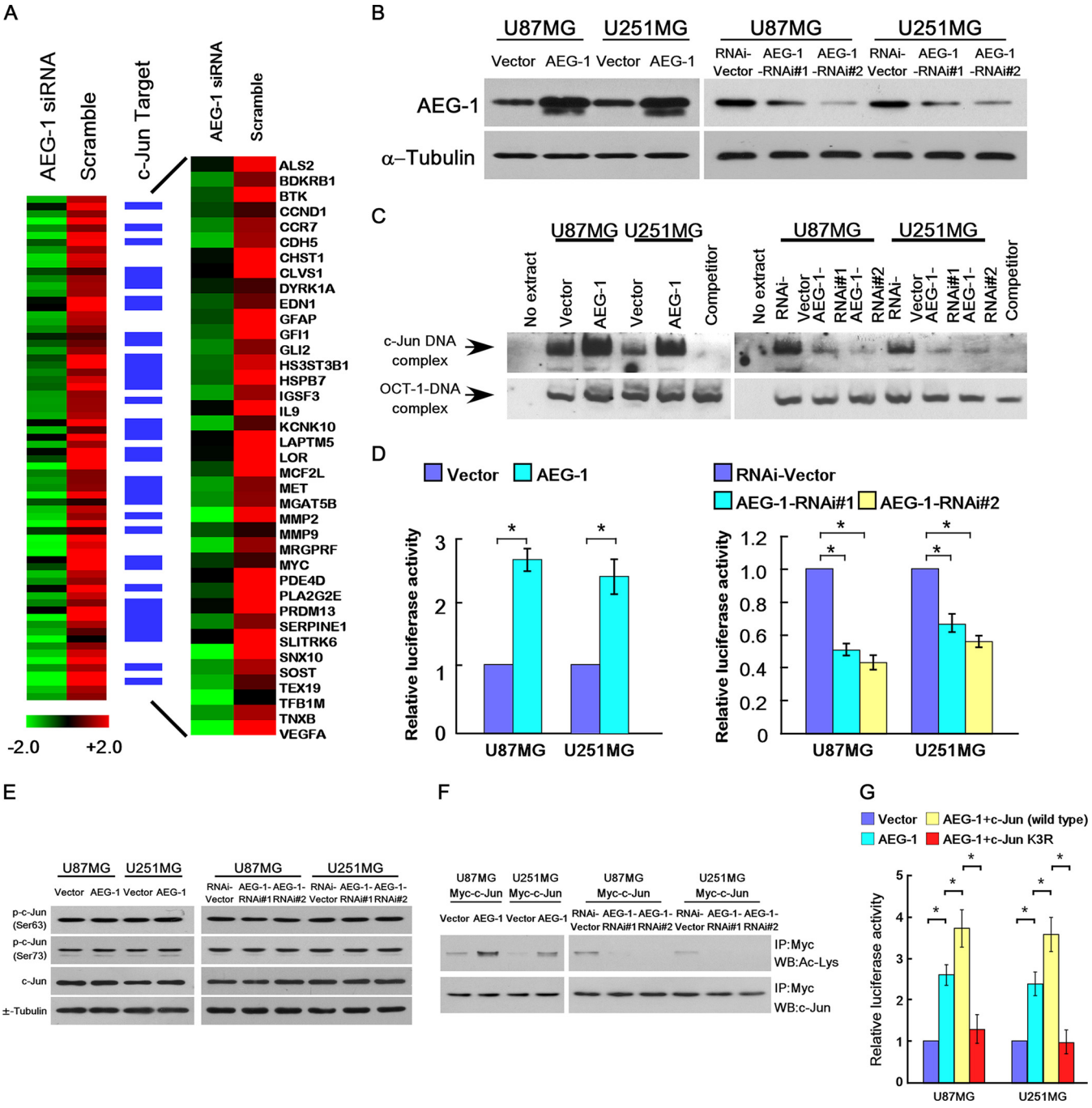

FIG 1 AEG-1 promotes c-Jun transactivation via acetylation. (A) Expression profile of U87MG cells transfected with AEG-1-specific siRNA or the scrambled siRNA control. (B) Ectopic expression of AEG-1 and knockdown of AEG-1 expression in the U87MG and U251MG glioma cell lines were analyzed by immunoblotting using an anti-AEG-1 antibody. α-Tubulin was utilized as the loading control. (C) Changes in the DNA-binding affinity of c-Jun in the indicated cells on the basis of the results of EMSA analysis. (D) Induction of c-Jun activity by AEG-1 overexpression and repression of c-Jun activity by AEG-1-RNAi in U87MG and U251MG glioma cells, as demonstrated using a luciferase activity assay. (E) Western blotting of levels of phosphorylated c-Jun (p-c-Jun) with phosphorylation at Ser63, phosphorylated c-Jun with phosphorylation at Ser73, and total c-Jun were examined in AEG-1-overexpressing or -knockdown cells. α-Tubulin was detected as a loading control. IP, immunoprecipitation. (F) Western blot analysis of acetylated c-Jun expression in the indicated cells. Ac, acetylated. (G) Changes in c-Jun activity in the indicated AEG-1-transfected cells transfected with wild-type c-Jun or the K3R-c-Jun mutant expression construct. The bars represent the mean values ± SDs obtained from three independent experiments. *, $P < 0.05$, Student's t test.

the effect of AEG-1 on c-Jun transactivation is associated with the increased acetylation of c-Jun.

AEG-1 interacts with c-Jun and p300. Since the transcriptional efficiency of c-Jun could be modulated by the p300 acetylation of c-Jun (20–22), we further investigated

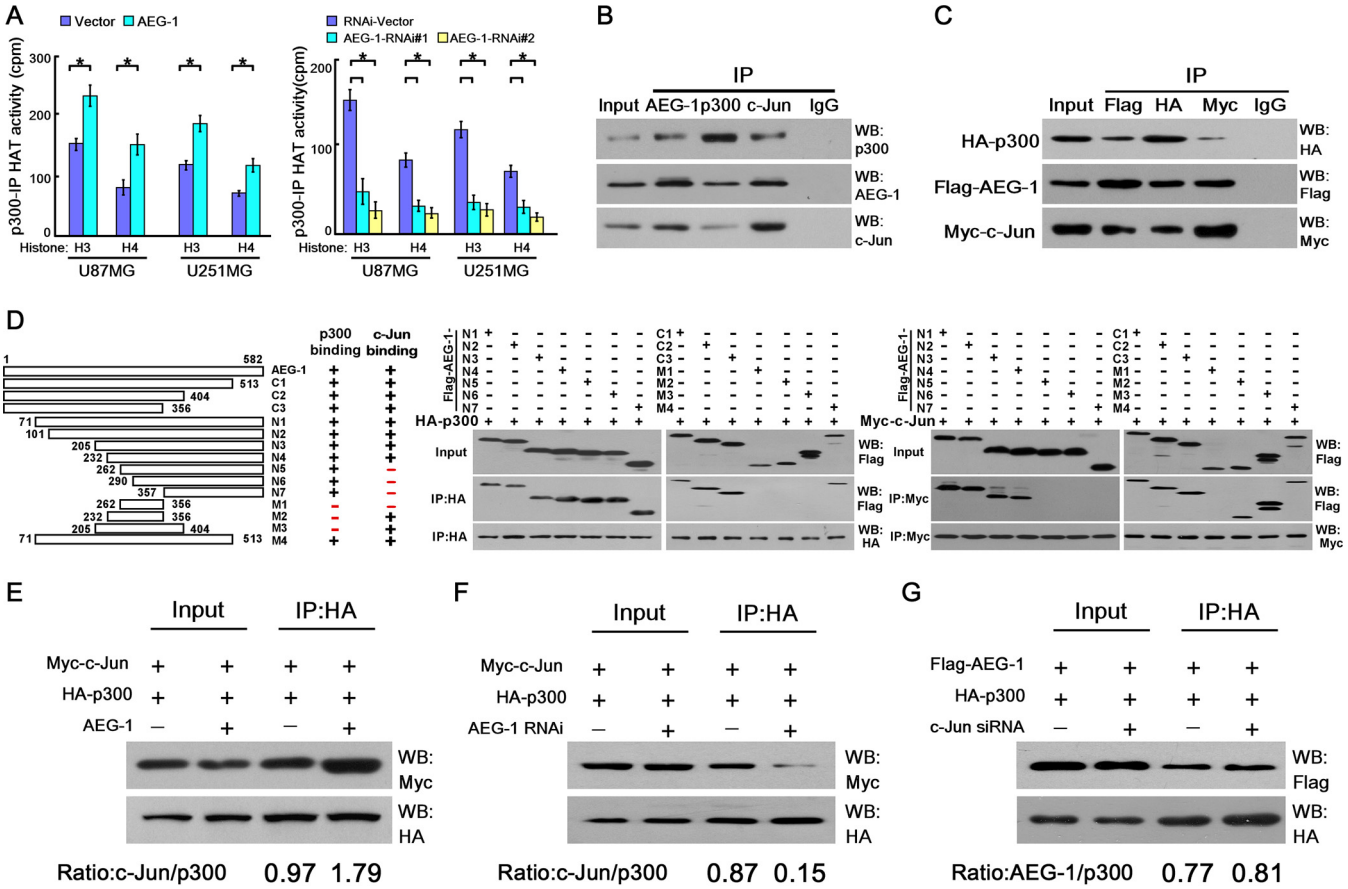

FIG 2 Identification of AEG-1 as a p300- and c-Jun-binding partner. (A) Acetyltransferase activity levels of p300 in the indicated cells, as determined by an increase in the radioactivity of synthetic histone H3 and H4 peptides (Millipore) by incubation with ^{3}H-labeled acetyl coenzyme A. (B) Association between endogenous AEG-1, p300, and c-Jun in U87MG cells. Proteins were immunoprecipitated from U87MG cell lysates using anti-AEG-1, anti-p300, or anti-c-Jun protein G-conjugated antibodies, after which immunoblotting was performed. (C) Association between ectopic Flag-tagged AEG-1, HA-tagged p300, and Myc-tagged c-Jun in U87MG cells. Proteins were immunoprecipitated from U87MG cells transfected with Flag-tagged AEG-1, HA-tagged p300, and Myc-tagged c-Jun using protein G-conjugated anti-Flag, anti-HA, or anti-Myc antibodies, followed by immunoblotting analysis. (D) (Left) Schematic illustrations of the constructs containing truncated AEG-1 fragments. The numbers indicate the positions of the terminal amino acid residues in each fragment. (Middle) Proteins were immunoprecipitated from lysates of HEK293 cells cotransfected with HA-p300 and Flag-tagged AEG-1 fragment constructs using anti-HA affinity agarose. (Right) Proteins were immunoprecipitated from HEK293 cell lysates cotransfected with Myc-c-Jun and Flag-tagged AEG-1 fragment constructs using anti-Myc affinity agarose. (E and F) Coimmunoprecipitation assay showing that overexpression of AEG-1 increased the extent of the interaction between p300 and c-Jun (E), whereas silencing of AEG-1 decreased the p300 and c-Jun interaction (F). (G) c-Jun knockdown has no effect on the interaction between AEG-1 and p300. The bars represent the mean values ± SDs obtained from three independent experiments. *, $P < 0.05$, Student's t test.

whether deregulated AEG-1 affects the acetyltransferase activity of endogenous p300 acetyltransferase. As shown in Fig. 2A, the level of p300 acetyltransferase activity was significantly higher in AEG-1-overexpressing cells than in control cells. In contrast, the level of endogenous p300 acetyltransferase activity was dramatically deceased in AEG-1-knockdown cells (Fig. 2A). Moreover, the results of a coimmunoprecipitation (co-IP) assay performed using an antibody directed against AEG-1 demonstrated that AEG-1 interacted with both p300 and c-Jun (Fig. 2B). Reciprocal co-IP assays using antibodies directed against p300 or c-Jun showed that AEG-1 coimmunoprecipitated with p300 and with c-Jun (Fig. 2B). Consistent with the observation in glioma cell lines, AEG-1 indeed interacts with both p300 and c-Jun in patient-derived glioma cells (Fig. S1A). These results was then further confirmed using cells ectopically expressing the three tagged proteins using agarose beads conjugated to antibodies directed against the tag epitopes (Fig. 2C). Additionally, amino-terminal (N) segments (N1 to N7), carboxyl-terminal (C) segments (C1 to C3), and middle segments (M4) of AEG-1 could be coimmunoprecipitated with hemagglutinin (HA)-tagged p300, whereas the middle portions of AEG-1 (M1, M2, and M3) did not interact with HA-tagged p300 (Fig. 2D). These data suggest that both the N terminus (amino acids [aa] 71 to 205) and the C

terminus (aa 404 to 513) of AEG-1 contribute to its interaction with p300. Moreover, although the amino-terminal (N) segments (N5 to N7) and middle segment (M1) fragments of AEG-1 could not be coimmunoprecipitated with Myc-tagged c-Jun, the amino-terminal (N) segments (N1 to N4), carboxyl-terminal (C) segments (C1 to C3), and middle segments (M2 to M4) of AEG-1 could be coimmunoprecipitated with Myc-tagged c-Jun (Fig. 2D), suggesting that the middle region (aa 232 to 262) of AEG-1 contributes to its interaction with c-Jun.

Furthermore, we found that the overexpression of AEG-1 promoted the interaction between p300 and c-Jun, whereas silencing of AEG-1 expression inhibited this interaction (Fig. 2E and F and S1B and C). However, the extent of the interaction between AEG-1 and p300 was not affected by c-Jun knockdown (Fig. 2G).

The AEG-1/p300/c-Jun complex binds to promoter/enhancer transcriptional activation regions. Because the acetylation of promoter or enhancer elements can play an important role in the transcriptional activation of the corresponding genes, we sought to investigate whether enhancing the level of AEG-1-meditated p300 acetyltransferase activity could increase the level of activation of chromatin modifications. We chose to analyze vascular endothelial growth factor (VEGF), a c-Jun target gene (23–25), the expression of which was significantly downregulated in AEG-1 siRNA-transfected cells (Fig. 1A). As shown in Fig. 3A, the level of VEGF expression was markedly increased in cells overexpressing AEG-1 and was decreased in cells subjected to AEG-1 silencing. Meanwhile, the expression of VEGF could be partially but not completely rescued by expressing c-Jun in cells in which AEG-1 was interrupted by RNA interference (RNAi) (AEG-1-RNAi cells) (Fig. S2A). Binding site prediction analysis performed using the TRANSFAC (version 4.0) program revealed four putative c-Jun-binding sites within the VEGF promoter (Fig. 3B). The results of chromatin immunoprecipitation (ChIP) assays revealed that AEG-1 bound the second and third potential c-Jun-binding sites within the VEGF promoter (Fig. 3C). The results of a dual-luciferase reporter assay showed that the luciferase activities driven by the VEGF promoter, covering segments of nucleotides -1140 to $+690$, -1700 to $+690$, and -2200 to $+690$, were increased in AEG-1-overexpressing cells compared with those in the control cells (Fig. 3D and E). Conversely, the luciferase activities driven by these segments of the VEGF promoter decreased in AEG-1-silenced cells (Fig. 3D and E). Furthermore, we evaluated whether the c-Jun-binding site in the VEGF promoter is essential for AEG-1-induced luciferase activation. As shown in Fig. 3F, the luciferase activities in AEG-1-overexpressing cells decreased when the second or third potential c-Jun-binding site within the VEGF promoter was mutated, suggesting that AEG-1 promotes VEGF promoter transactivation through second and third potential c-Jun-binding sites.

As shown in Fig. 3G, the enrichment of AEG-1 and p300 binding within the VEGF promoter was significantly reduced when c-Jun was knocked down. Moreover, AEG-1 silencing reduced the DNA-binding affinities of both p300 and c-Jun to AEG-1-bound c-Jun target sites (Fig. 3H). Furthermore, our results showed a significant decrease in the levels of acetylated histones H3 and H4 in parallel with increased levels of histone deacetylase 1/3 (HDAC1/3) recruitment at the putative c-Jun-binding sites upon AEG-1 knockdown (Fig. 3I). Moreover, expression of c-Jun in AEG-1-RNAi cells could partially rescue the levels of acetylated histones H3 and H4 at the putative c-Jun-binding sites in the VEGF promoter (Fig. S2B). These results provide additional support for the hypothesis that AEG-1 plays an essential role in establishing an acetylated chromatin state that favors transcriptional activation.

AEG-1-mediated c-Jun acetylation promotes cancer progression. We next determined whether AEG-1-mediated c-Jun acetylation contributes to the development of malignant properties in gliomas. As shown in Fig. 4A, human umbilical vein endothelial cells (HUVECs) cultured in conditioned medium (CM) transferred from AEG-1-overexpressing cells formed significantly larger numbers of capillary-like structures than the vector controls, whereas HUVECs cultured in CM derived from cultured AEG-1-knockdown cells formed fewer capillary-like structures, suggesting that AEG-1 pro-

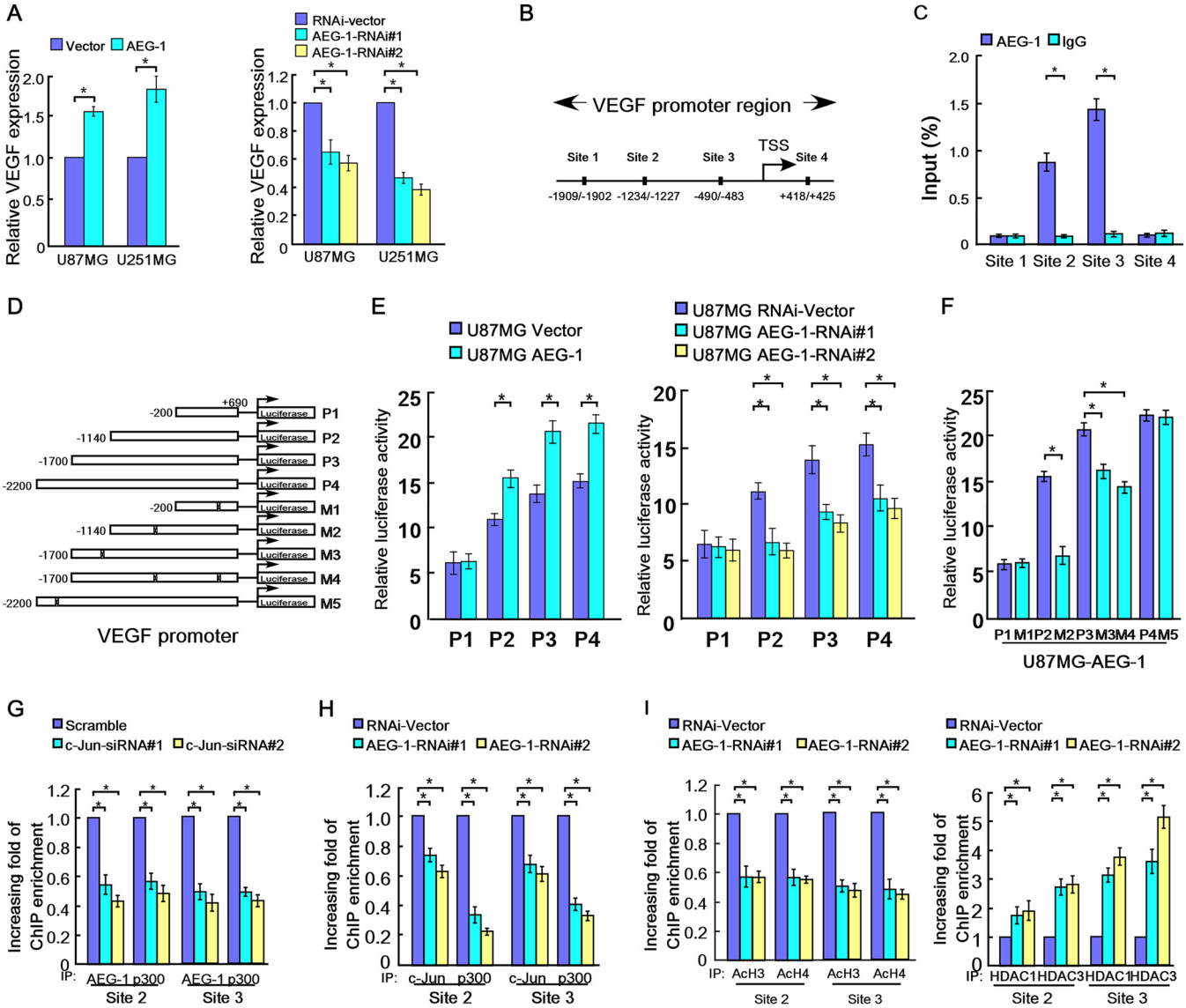

FIG 3 AEG-1 establishes an acetylated chromatin state that favors transcriptional activation. (A) Levels of VEGF secretion by the indicated cells, as determined by ELISA. (B) Schematic illustration showing four deduced c-Jun-binding sites within the VEGF promoter. TSS, transcription start site. (C) ChIP assay results showing AEG-1 enrichment at the second and third c-Jun-binding sites within the VEGF promoter. (D) Schematic illustration of the truncated VEGF promoter constructs and the constructs with mutated c-Jun-binding sites. (E) Levels of transactivating activity of serial VEGF promoter fragments in the indicated U87MG cells. (F) Levels of transactivation activity of serial VEGF promoter fragments and the corresponding fragments with mutant c-Jun-binding sites in U87MG cells overexpressing AEG-1. (G) Levels of enrichment of AEG-1 and p300 on the AEG-1-bound c-Jun-binding sites in the indicated cells, determined by ChIP assay. (H) Levels of enrichment of c-Jun and p300 on AEG-1-bound c-Jun-binding sites in the indicated cells, determined by ChIP assay. (I) Levels of enrichment of acetylated histones H3 and H4, HDAC1, and HDAC3 at AEG-1-bound c-Jun-binding sites in the indicated cells, determined by ChIP assay. The bars represent the mean values ± SDs obtained from three independent experiments.*, $P < 0.05$, Student's *t* test.

voked the angiogenesis-inducing ability of glioma cells. Moreover, we found that the proangiogenic effects of AEG-1 on glioma cells could be abrogated by overexpression of the dominant negative K3R-c-Jun mutant (Fig. 4B). Colony formation and 3-(4,5-dimethyl-2-thiazolyl)-2,5-diphenyl-2H-tetrazolium bromide (MTT) assays showed that overexpression of AEG-1 promoted the propagation of glioma cells, whereas AEG-1 depletion inhibited the propagation of glioma cells (Fig. 4C and E). Furthermore, the expression of the K3R-c-Jun mutant markedly inhibited the AEG-1-induced proliferation of glioma cells (Fig. 4D and F). Taken together, these data obtained using glioma cells as a model reveal the effects of AEG-1-mediated c-Jun acetylation on tumor neovascularization and proliferation.

Additionally, *in vivo* animal experiments were performed to examine the effect of AEG-1-dependent c-Jun acetylation on tumor progression. Using a flank xenograft

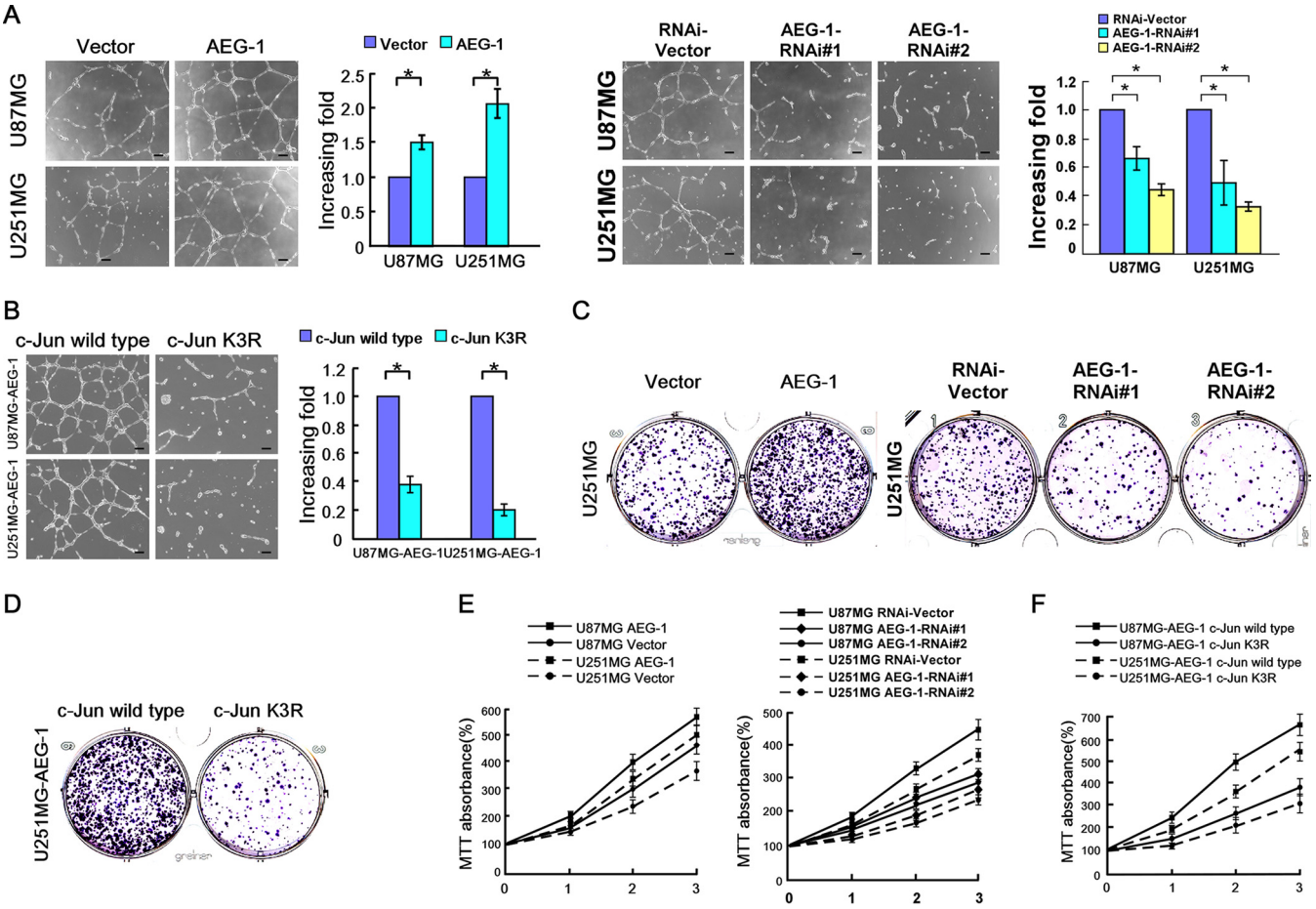

FIG 4 AEG-1 enhances angiogenesis and cell proliferation in a c-Jun acetylation-dependent manner. (A and B) Representative images (left) and quantification (right) of tubules formed by HUVECs cultured on Matrigel-coated plates with medium conditioned by blank vector-transfected, AEG-1-overexpressing, AEG-1-silenced cells (A) or AEG-1-overexpressing cells transfected with wild-type c-Jun or the K3R-c-Jun mutant (B). Bars, 100 μm. (C and D) Colony formation by empty vector-transfected, AEG-1-overexpressing, AEG-1-silenced cells (C) or AEG-1-overexpressing cells transfected with wild-type c-Jun or the K3R-c-Jun mutant (D). (E) The results of the MTT assay indicate that ectopic expression of AEG-1 enhances glioma cell proliferation (left) but knockdown of AEG-1 reduces glioma cell proliferation (right). *x* axis, time in days. (F) Results of the MTT assay showing that the K3R-c-Jun mutant inhibits AEG-induced glioma cell proliferation. *x* axis, time in days. The error bars represent the mean values ± SDs from three independent experiments. *, $P < 0.05$, Student's *t* test.

tumor model, we found that tumors formed by cells overexpressing AEG-1 grew faster than those formed by control cells, whereas cells with stable knockdown of AEG-1 formed relatively smaller tumors (Fig. 5A). Furthermore, the tumor-promoting activity of AEG-1 could be blocked by K3R-c-Jun expression (Fig. 5A). As shown in Fig. 5B, the tumors formed by AEG-1-overexpressing glioma cells in the brains of nude mice were far larger and displayed markedly increased levels of CD31 and higher levels of Ki67 signals compared with the ones formed by vector control cells. Moreover, the tumors formed by AEG-1-overexpressing glioma cells transfected with the K3R-c-Jun mutant exhibited a smaller size and reduced CD31 and Ki67 staining compared with those formed by AEG-1-overexpressing cells or AEG-1-overexpressing cells transfected with wild-type c-Jun. These data suggest an important role of c-Jun acetylation in mediating these AEG-1-induced biological effects.

Clinical relevance of the c-Jun transcriptional targets that are regulated by AEG-1 in human gliomas. Finally, we examined whether the experimentally observed AEG-1-mediated c-Jun activation is clinically relevant for human gliomas. Immunohistochemistry (IHC) analysis of 149 glioma clinical specimens revealed that the level of AEG-1 was significantly correlated with the expression of markers of glioma aggressiveness, such as those of the endothelial marker CD31 ($P < 0.001$) and the proliferative marker Ki67 ($P < 0.001$), as well as with the levels of expression of c-Jun downstream

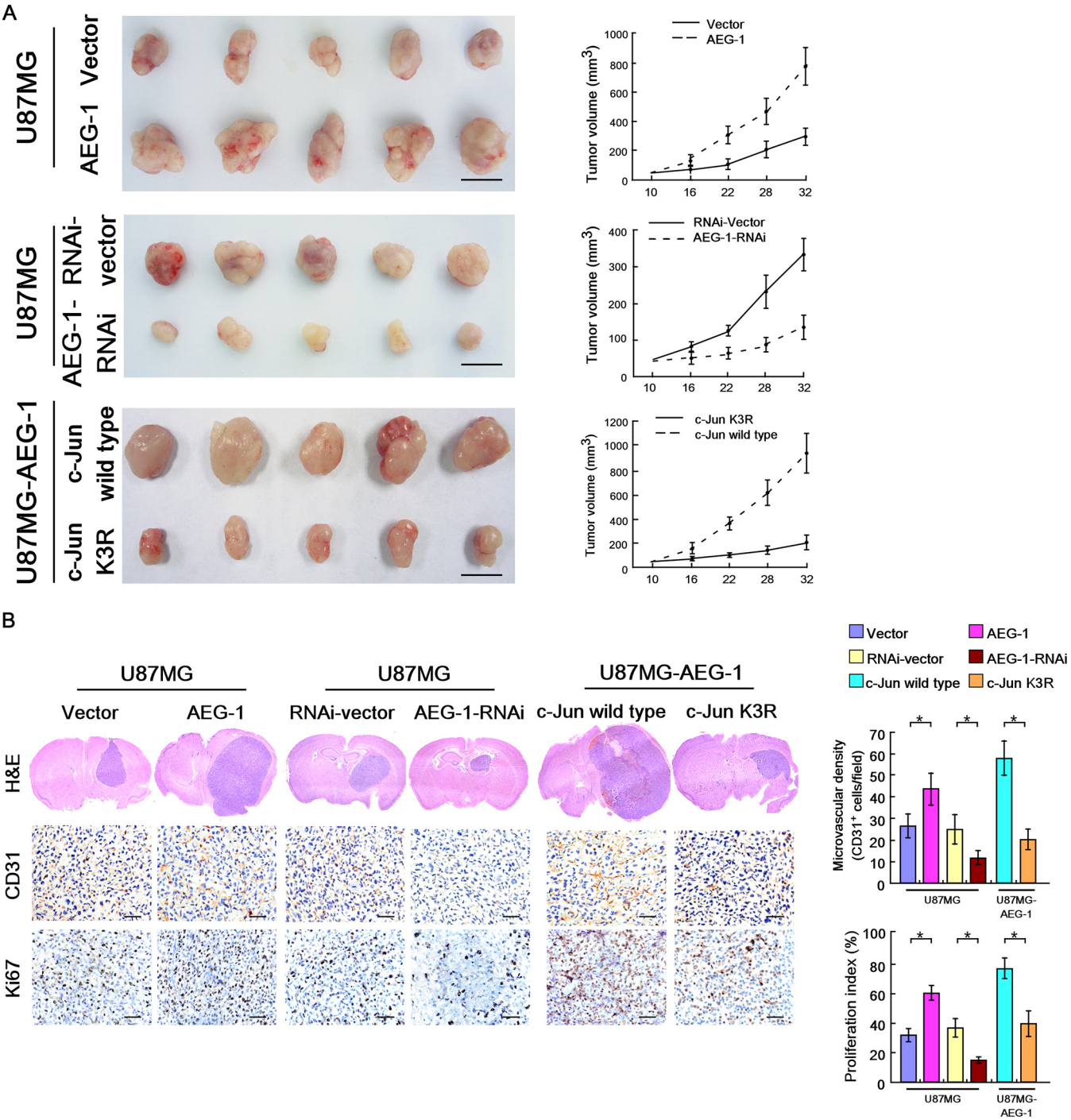

FIG 5 AEG-1 enhances acetylation-dependent angiogenesis and tumor growth *in vivo*. (A) Representative graphs of the tumor diameters (left) and tumor volumes determined at the indicated time points (days) (right). The indicated cells (5×10^6) were injected into the two flanks of each nude mouse. Bars, 1 cm. The bars represent the mean values ± SDs ($n = 5$ mice per group). (B) H&E and IHC staining for CD31 and Ki67 in tumors formed by the indicated glioma cells in the brains of nude mice. *, $P < 0.05$, Student's *t* test.

gene transcripts, including those of VEGF ($P < 0.001$), c-MET ($P < 0.001$), cyclin D1 ($P < 0.001$), and MMP-2 ($P < 0.001$) (Fig. 6A and B). In addition, EMSA results showed that the level of AEG-1 expression was strongly associated with the level of c-Jun transcriptional activity ($r = 0.762$, $P = 0.028$) (Fig. 6C and D). Taken together, these data demonstrate the importance of AEG-1 overexpression for the induction of the expression of c-Jun downstream genes and for the promotion of glioma aggressiveness.

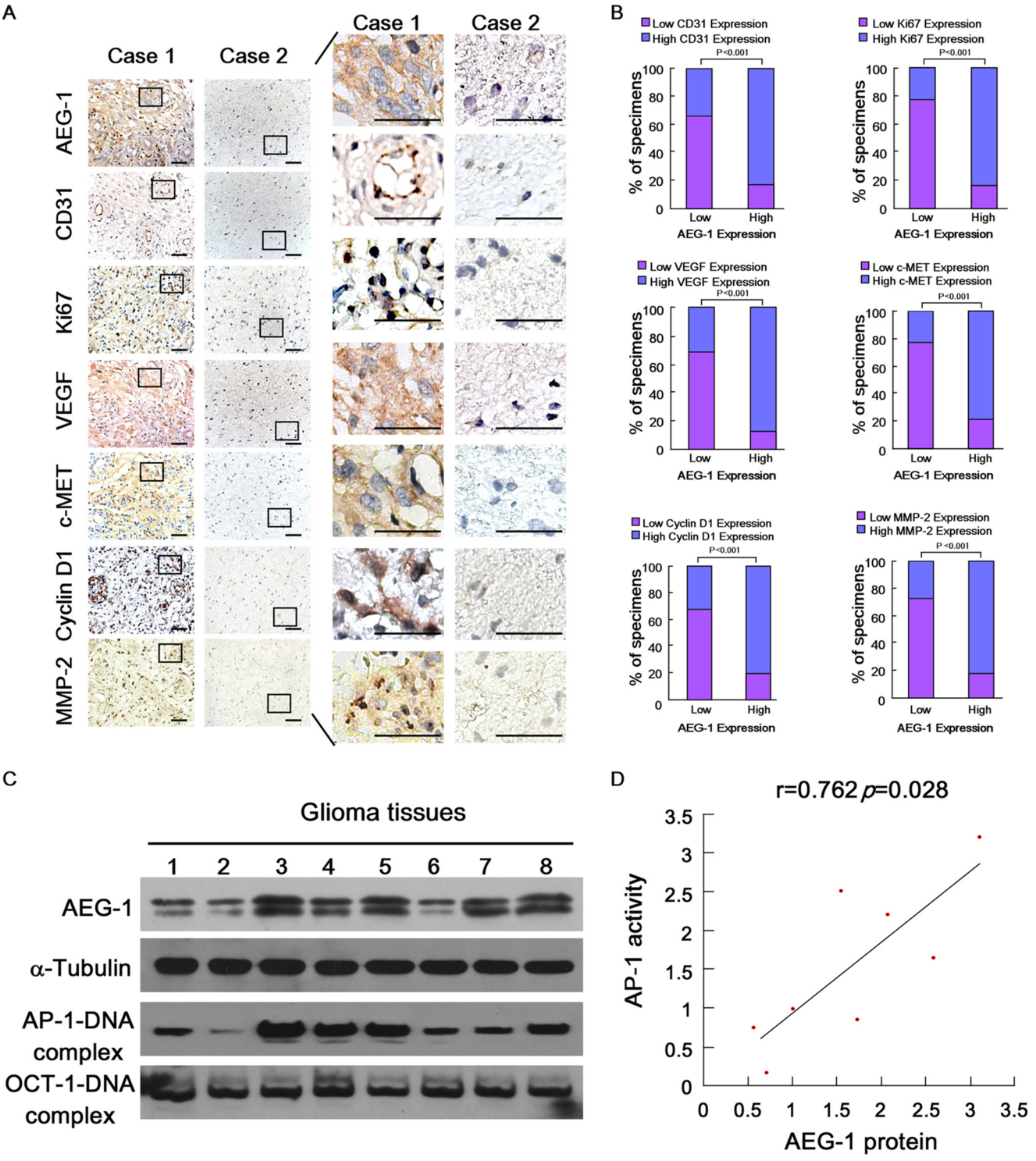

FIG 6 Clinical relevance of AEG-1-induced c-Jun activation in human gliomas. (A) The AEG-1 expression level is associated with the level of CD31, Ki67, VEGF, c-MET, cyclin D1, or MMP-2 expression in a cohort of 149 human glioma specimens. The results for two representative cases are shown. The boxed regions in the two left columns are enlarged in the two right columns. Bars, 50 μm. (B) Percentages of specimens showing low- or high-level AEG-1 expression relative to the levels of CD31, Ki67, VEGF, c-MET, cyclin D1, or MMP-2 expression, which were determined by IHC. (C and D) Correlation between the c-Jun expression and c-Jun activity.

To identify a c-Jun signaling pathway that was strongly associated with AEG-1 expression, gene set enrichment analysis (GSEA) was conducted. As shown in Fig. 7A, the GSEA results obtained using tumor samples from glioblastoma patients that were deposited in The Cancer Genome Atlas (TCGA) data set (n = 605) showed a marked

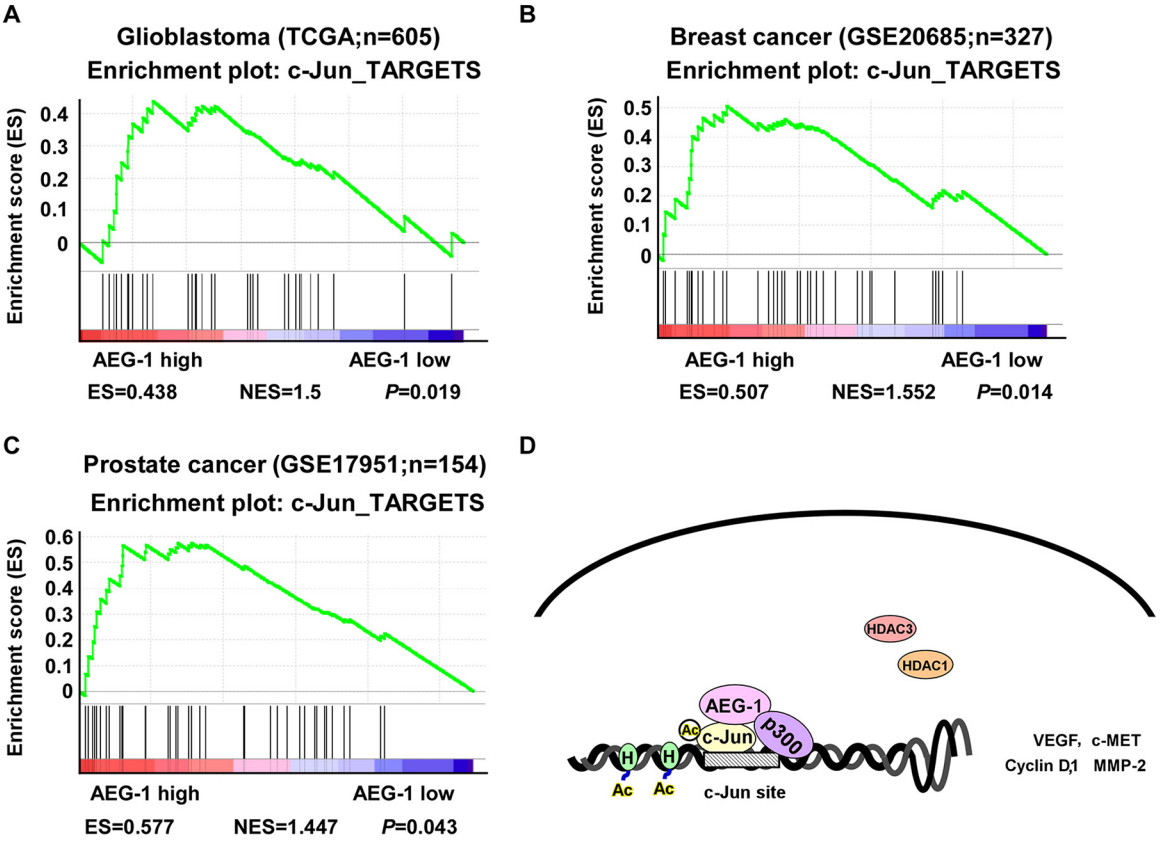

FIG 7 Relationship between the AEG-1 expression signatures and the c-Jun-activated gene signatures, as analyzed by GSEA. (A) GSEA plots of the AEG-1 expression signatures and the c-Jun-activated gene signatures of glioblastoma patients, obtained from the TCGA database (n = 605). (B) GSEA plots of the AEG-1 expression signatures and the c-Jun-activated gene signatures observed in breast cancer data sets (Gene Expression Omnibus database accession number GSE20685; n = 327). (C) GSEA plots of the AEG-1 expression signatures and the c-Jun-activated gene signatures observed in prostate cancer data sets (Gene Expression Omnibus database accession number GSE17951; n = 154). (D) Schematic model of AEG-1-dependent acetylation and activation of c-Jun in a glioma.

enrichment in the levels of AP-1-activated gene expression in high-grade glioblastoma tumors expressing AEG-1 (enrichment score [ES] = 0.438; normalized enrichment score [NES] = 1.5; P = 0.019). The levels of c-Jun-activated gene signatures were markedly enriched in the breast cancer group expressing high levels of AEG-1, as analyzed using GSEA of the relevant data sets (Gene Expression Omnibus database accession number GSE20685; P = 0.014), and in the prostate cancer data sets (Gene Expression Omnibus database accession number GSE17951; P = 0.043) (Fig. 7B and C). Together, these results further support the hypothesis that AEG-1 binds p300 and c-Jun and enhances the acetylation of c-Jun, leading to the activation of the AP-1 signaling pathway and the enhancement of transcription of AP-1 target genes (Fig. 7D).

DISCUSSION

As the transcriptional hub of multiple upstream oncogenic signals, c-Jun transcription factors have been found to be constitutively activated in many types of tumors (26–28) and to participate in various processes that promote tumor development and progression, such as angiogenesis and cell survival (29–32). The essential role of c-Jun in the progression of gliomas has been demonstrated in previous studies (33). Therefore, delineating the regulatory roles of c-Jun in cancer cells is of great importance. Posttranslational modifications of c-Jun, such as its phosphorylation and acetylation, are important regulatory factors involved in the transactivation of c-Jun (20–22). Driven by the activation of oncoproteins such as epidermal growth factor receptor (34) and Jun N-terminal protein kinase (29, 31, 35) or by the inactivation of the tumor suppressor PTEN (36), the phosphorylation of c-Jun (mainly at Ser63/Ser73) increases in a transient,

pulse-like fashion as the cell cycle progresses or in response to treatment with a mitogen or 12-*O*-tetradecanoylphorbol-13-acetate (37). In contrast, mutation of the K271 acetylation site of c-Jun and the flanking lysine residue results in the blockage of its transactivation activity even in the presence of mitogens (20), suggesting that the activation of c-Jun may require not only phosphorylation but also acetylation. In the current study, we found that overexpression of AEG-1 significantly increased the level of c-Jun acetylation and drove its transactivation activity. A c-Jun acetylation site mutant (K3R-c-Jun), which blocks acetylation-dependent AP-1 transactivation (20, 22), drastically diminished the stimulatory effect of AEG-1 on the transactivational activity of AP-1. These results provide new insights into the mechanisms underlying the oncogenic modulatory activity of c-Jun in cancer cells.

AEG-1 has been detected in various intracellular compartments and has been shown to possess pleiotropic properties. One important function of AEG-1 is to serve as a scaffold protein to mediate the formation of multiprotein complexes, thereby contributing to the regulation of diverse signaling pathways. In the cytoplasm, AEG-1 interacts with SND1, a component of the RNA-induced silencing complex (RISC), thus contributing to the onco-microRNA-mediated degradation of tumor suppressor mRNAs (10–12). In the nucleus, AEG-1 functions as a transcriptional coactivator by directly interacting with the p65 subunit of NF-κB and by functioning as a transcriptional repressor through its interaction with the promyelocytic leukemia zinc finger, thereby increasing the level of c-Myc transcription (7–9). These findings, together with the results obtained in the present study, suggest that AEG-1 is a key contributor to cancer development and progression by regulating the activity of several signaling cascades in different cellular compartments.

The results of this study demonstrate the essential role of AEG-1 in promoting c-Jun activity by interacting with p300 and c-Jun, which results in the subsequent acetylation of c-Jun. Notably, AEG-1 is a lysine-rich highly basic protein (15). Therefore, further investigation into whether its interaction with p300 results in the acetylation of AEG-1, which could lead to the occurrence of posttranslational modifications that modulate the biological effects of AEG-1, is of great interest.

In our current study, we identified AEG-1 to be a novel interacting partner of c-Jun and demonstrated that these interactions promote c-Jun activation. In a similar context, the activation of specific c-Jun complexes has been shown to be involved in the regulation of cellular death/survival in neurodegenerative diseases, possibly mediated through various signal transduction pathways, depending on different c-Jun-binding partners (38). Thus, the AEG-1/c-Jun interaction observed in glioma may also exist in neurodegenerative processes, implicating that AEG-1 may affect neurological integrity.

In summary, although previous publications have illustrated the multifunctional oncogenic characteristics of AEG-1, our results provide details of the mechanism involved in driving dysregulated c-Jun activity in human gliomas. We found that the interaction among AEG-1, p300, and c-Jun could play an important role in regulating c-Jun transcriptional activity, which could result in the development of a more aggressive phenotype of human glioma cells *in vitro* and *in vivo*. Our results suggest that a novel and promising therapeutic anticancer strategy could involve the targeting of AEG-1 to inhibit the aberrant function of acetyltransferases.

MATERIALS AND METHODS

Cell lines. The U87MG and U251MG glioma cell lines were kindly provided by Shi-Yuan Cheng (University of Pittsburgh, Pittsburgh, PA) and were grown in Dulbecco's modified Eagle medium (DMEM; Gibco, Thermo Fisher Scientific, Waltham, MA) supplemented with 10% fetal bovine serum (HyClone, Logan, UT) at 37°C with 5% CO_2. The authenticity of the cell lines was verified by short tandem repeat fingerprinting by the Medicine Laboratory of the Forensic Medicine Department of Sun Yat-sen University (Guangzhou, China).

Tissue specimens and patient information. A total of 149 paraffin-embedded, archived specimens in which glioma was clinically and histopathologically diagnosed at the First Affiliated Hospital of Sun Yat-sen University from 2000 to 2005 were used. The clinicopathological characteristics of the samples are summarized in Table 1. Fresh brain tumor tissue samples obtained from the First Affiliated Hospital of Sun Yat-sen University were collected and processed within 30 min after resection. Prior donor consent

TABLE 1 Clinicopathological characteristics of glioma samples

Characteristic	No. (%) of patients
Gender	
Male	101 (67.8)
Female	48 (32.2)
Age (yr)	
≤35	77 (51.7)
>35	72 (48.3)
Glioma histology (WHO grade)	
I	19 (12.8)
II	54 (36.2)
III	52 (34.9)
IV	24 (16.1)
Survival	
Alive	61 (40.9)
Dead	88 (59.1)

and study approval by the Institutional Research Ethics Committee of Zhongshan School of Medicine, Sun Yat-sen University, were obtained for our study.

Plasmids, retroviral infection, and transfection. Human AEG-1 was amplified by PCR and was cloned into the pMSCV-puro retroviral vector. Knockdown of endogenous AEG-1 was performed by cloning two short hairpin RNAs (shRNAs) using the following oligonucleotides: oligonucleotide 1 (AACAGAAGAAGAAGAACCGGA) and oligonucleotide 2 (GAAATCAAAGTCAGATGCTA) (synthesized at Invitrogen) into the pSuper-retro-puro vector to generate pSuper-retro-AEG-1-RNAis (AEG-1-RNAi#1 and AEG-1-RNAi#2, respectively). Fragments of the human AEG-1-coding sequence, which were generated by PCR amplification, were cloned into the pMSCV-puro retroviral vector. Different segments of the human VEGF promoter, including fragments covering nucleotides −200 to +690, −1140 to +690, −1700 to +690, and −2200 to +690 (numbered in relation to the transcription initiation site), were generated by PCR amplification using U87MG cell DNA as the template. Each of the products was cloned into the pGL3-basic luciferase reporter plasmid (Promega, Madison, WI). Mutations in the promoter segments were created using primers and a Stratagene mutagenesis kit according to the protocol recommended by the manufacturer. The sequences of all primers used for plasmids construction and site-specific mutagenesis are listed in the Tables 2 and 3, respectively. Small interfering RNA (siRNA) duplexes were synthesized and purified by Ribobio Inc. (Guangzhou, Guangdong, China). The sequences of the siRNAs used were as follows: for AEG-1 siRNA, 5′-AACAGAAGAAGAAGAACCGGA-3′; for c-Jun siRNA#1, 5′-CGC AGCAGTTGCAAACATT-3′; and for c-Jun siRNA#2, 5′-GACCTTATGGCTACAGTAA-3′. Transfection of the siRNAs was performed using the Lipofectamine 2000 reagent (Invitrogen, Carlsbad, CA) according to the instructions recommended by the manufacturer.

TABLE 2 Primers used for Flag-tagged AEG-1 fragment plasmid construction

Primer	Sequence
AEG-1-N1-up	CGCGGATCCGCCATGTGGGCCGCGGCTTGCGCCGGCTC
AEG-1-N2-up	CGCGGATCCGCCATGGACGACCTGGCCTTGCTGAAGAATC
AEG-1-N3-up	CGCGGATCCGCCATGCGTAAACGTGATAAGGTGCTGACTG
AEG-1-N4-up	CGCGGATCCGCCATGACCGAGCAACTTACAACCGCATC
AEG-1-N5-up	CGCGGATCCGCCATGTCTGGAAAAGGAGATTCTACACTTC
AEG-1-N6-up	CGCGGATCCGCCATGTCTGTAAAACTCTCCTCACAGATC
AEG-1-N-dn	TGCTCTAGATCACTTGTCATCGTCGTCCTTGTAGTCCGTTTCTCGTCTGGCTTTTTTC
AEG-1-N7-up	CGCGGATCCGCCATGGACTACAAGGACGACGATGACAAGCAGTCTACCACTTCTGATTA
AEG-1-N7-dn	CCGGAATTCTCACGTTTCTCGTCTGGCTTTTTTC
AEG-1-C-up	CGCGGATCCGCCATGGCTGCACGGAGCTGGCAGGACGAG
AEG-1-C1-dn	TGCTCTAGATCACTTGTCATCGTCGTCCTTGTAGTCAAGAGTCTTGATAGGCTGGC
AEG-1-C2-dn	TGCTCTAGATCACTTGTCATCGTCGTCCTTGTAGTCCCAATTGCCCCACTCTTCTG
AEG-1-C3-dn	TGCTCTAGATCACTTGTCATCGTCGTCCTTGTAGTCAACTGGCTCAGCAGTAGACC
AEG-1-M1-up	CGCGGATCCGCCATGGACTACAAGGACGACGATGACAAGGGAAAAGGAGATTCTACAC
AEG-1-M1-dn	CCGGAATTCTCAAACTGGCTCAGCAGTAGACCC
AEG-1-M2-up	CGCGGATCCGCCATGGACTACAAGGACGACGATGACAAGGAGCAACTTACAACCGCATC
AEG-1-M2-dn	CCGGAATTCTCAAACTGGCTCAGCAGTAGACCC
AEG-1-M3-up	CGCGGATCCGCCATGGACTACAAGGACGACGATGACAAGCGTAAACGTGATAAGGTGC
AEG-1-M3-dn	CCGGAATTCTCACCAATTGCCCCACTCTTCTGC
AEG-1-M4-up	CGCGGATCCGCCATGGACTACAAGGACGACGATGACAAGTGGGCCGCGGCTTGCGCCGG
AEG-1-M4-dn	CCGGAATTCTCATGGAAGAGTCTTGATAGGCTGGC

TABLE 3 Primers used for luciferase reporter plasmid and site mutation

Primer	Sequence
7×AP-1-Luc-up	CGCGTTGACTAATGACTAATGACTAATGACTAATGACTAATGACTAATGACTAAA
7×AP-1-Luc-dn	GATCTTTAGTCATTAGTCATTAGTCATTAGTCATTAGTCATTAGTCATTAGTCAA
VEGF-Luc-P1-up	GCCGGTACCAGGACAGTTGGCTTATGG
VEGF-Luc-P1-dn	GGCAAGCTTCCCAGTTCCATCGGTATG
VEGF-Luc-P2-up	GCCGGTACCAACCACAGCAACATGTG
VEGF-Luc-P2-dn	GGCAAGCTTCAGCACTAAGGAACGTC
VEGF-Luc-P3-up	TGCGGTACCGCGGGTAGGTTTGAATC
VEGF-Luc-P3-dn	GGCAAGCTTCCCACCAAGGTTCACAG
VEGF-Luc-P4-up	TGAGGTACCGAGCTTCCCCTTCATTGC
VEGF-Luc-P4-dn	CCAAAGCTTGAAGCGAGAACAGCCCAG
VEGF-Luc-Mut1-up	GGCCTGCCTGGGAGGGGGCCCTGAGTTTGGAAATAAACATTTACTAACTG
VEGF-Luc-Mut1-dn	CAGTTAGTAAATGTTTATTTCCAAACTCAGGGCCCCCTCCCAGGCAGGCC
VEGF-Luc-Mut2-up	CCCCCATTTCTATTCAGAAGATGAGAAATGAGAAAGGGCTTGGGCTGATAGAAGCCTTG
VEGF-Luc-Mut2-dn	CAAGGCTTCTATCAGCCCAAGCCCTTTCTCATTTCTCATCTTCTGAATAGAAATGGGGG
VEGF-Luc-Mut3-up	CTGTGTGGGTGAGTGAGAAAGTGCGTGTGGGGTTGAG
VEGF-Luc-Mut3-dn	CTCAACCCCACACGCACTTTCTCACTCACCCACACAG
VEGF-Luc-Mut5-up	GGGACAGGGGCAAAGTGAGAAACCTGCTTTTGGGGGT GAC
VEGF-Luc-Mut5-dn	GTCACCCCCAAAAGCAGGTTTCTCACTTTGCCCCTGTC CC
c-Jun-K3R-up	CCGCATCGCTGCCTCCCGGTGCCGACGAAGGCGGCTGGAGAGAATCGCCCG
c-Jun-K3R-dn	CGGGCGATTCTCTCCAGCCGCCTTCGTCGGCACCGGGAGGCAGCGATGCGG

Western blot analysis. Western blotting (WB) was performed as previously described (39) using an anti-AEG-1 antibody (1:1,000; catalog number 40-6500; Thermo Fisher Scientific), an anti-p300 antibody (1:500; catalog number 05-257; Merck Millipore, Billerica, MA), an anti-c-Jun antibody (1:1,000; catalog number 9165; Cell Signaling, Danvers, MA), an anti-phospho-c-Jun antibody (Ser 63) (1:1,000; catalog number 9261; Cell Signaling), an anti-phospho-c-Jun (Ser73) antibody (1:1,000; catalog number 3270; Cell Signaling), an anti-acetyl lysine antibody (1:500; catalog number ab21623; Abcam, Cambridge, MA), an anti-HA tag antibody (1:5,000; catalog number H9658; Sigma, St. Louis, MO), an anti-Flag tag antibody (1:5,000; catalog number F3165; Sigma), and an anti-Myc tag antibody (1:5,000; catalog number ab9132; Abcam). After the initial Western blotting assay was performed, the membranes were stripped and were reprobed with an anti-α-tubulin antibody (1:1,000; catalog number T9026; Sigma) to determine the levels of the loading control.

Luciferase assay. Three thousand cells were seeded in triplicate in 48-well plates and were incubated for 24 h. One hundred nanograms of the luciferase reporter plasmid or the control luciferase plasmid plus 1 ng of the pRL-TK *Renilla* plasmid (Promega) were transfected into glioma cells using the Lipofectamine 2000 reagent (Invitrogen, Carlsbad, CA) according to the protocol recommended by the manufacturer. The luciferase and *Renilla* signals were measured 24 h after transfection using a dual-luciferase reporter assay kit (Promega) according to the manufacturer's instruction. Three independent experiments were performed. The data are presented as the mean values ± standard deviations (SDs).

HUVEC tubule formation assay. Human umbilical vein endothelial cells (HUVECs) were purchased from ATCC (Manassas, VA) and were cultured according to the protocol recommended by the manufacturer. Matrigel (BD Biosciences, Bedford, MA) was pipetted into each well of a 24-well plate and was allowed to polymerize for 30 min at 37°C. HUVECs (2×10^4) in 200 μl of conditioned medium were added to each well, and the plate was incubated at 37°C with 5% CO_2 for 20 h. Photographs were taken under a bright-field microscope (magnification, ×100), and the total lengths of the completed capillary tubular structures were measured. The effect of each experimental condition was assessed at least in triplicate.

ELISA. The concentrations of VEGF in the cell-conditioned medium were determined using a commercially available VEGF-specific enzyme-linked immunosorbent assay (ELISA) kit (Keygen Co. Ltd., Nanjing, China). The ELISA was performed according to the protocol recommended by the manufacturer. Briefly, the conditioned medium was added to a well coated with a VEGF polyclonal antibody, and then a biotinylated monoclonal anti-human VEGF antibody was added and the plate was incubated at room temperature for 2 h. The color development catalyzed by horseradish peroxidase was terminated using 2.5 M sulfuric acid, and the absorption at 450 nm was measured. The protein concentration was determined by comparing the absorbance levels of the samples with those of the standards.

p300-HAT activity. The level of p300-histone acetyltransferase (p300-HAT) activity was determined using an immunoprecipitation-HAT assay kit (catalog number 17-284; Merck Millipore). Briefly, endogenous p300 was precipitated using 5 μg of an anti-p300 antibody (Merck Millipore), and the immunoprecipitate was subsequently incubated with histone H4 peptide and ^{3}H-labeled acetyl coenzyme A. The level of HAT activity was determined on the basis of the substrate radioactivity, which was measured using a liquid scintillation counter.

Chromatin immunoprecipitation (ChIP). Cells (2×10^6) plated in a 100-mm culture dish were treated with 1% formaldehyde to cross-link the proteins to the DNA. The cell lysates were sonicated to shear the DNA into fragments of 300 bp to 1,000 bp. Equal aliquots of the chromatin supernatants were incubated with 1 μg of an anti-AEG-1 antibody (catalog number 40-6500; Thermo Fisher Scientific), an anti-c-Jun antibody (catalog number 9165; Cell Signaling), an anti-p300 antibody (catalog number 05-257; Merck Millipore), an anti-acetyl-histone H3 antibody (catalog number 17-615; Merck Millipore), an

anti-acetyl-histone H4 antibody (catalog number 17-630; Merck Millipore), an anti-HDAC1 antibody (catalog number ab7028; Abcam), or an anti-HDAC3 antibody (catalog number ab7030; Abcam) overnight at 4°C with rocking. As a negative control, an anti-IgG antibody (catalog number ab172730; Abcam) was used to ensure antibody specificity. After reverse cross-linking of the protein/DNA complexes to free the DNA, PCR was performed using the following specific primers: for site 1, forward primer 5′-GTTCA TCAGCCTAGAGCATG-3′ and reverse primer 5′-ATCATTCGTGCACTAGTCCT-3′; for site 2, forward primer 5′-CGAAACCCCCATTTCTATTCAG-3′ and reverse primer 5′-ACCCGCCAGCACTAAGGAA-3′; for site 3, forward primer 5′-ATGGAGCGAGCAGCGTCTT-3′ and reverse primer 5′-CCTTCTCCCCGCTCCAA-3′; and for site 4, forward primer 5′-AAGAGGTAGCAAGAGCTCCAGAGA-3′ and reverse primer 5′-GGCGGTCACCCCC AAA-3′.

Coimmunoprecipitation. Cells grown in 100-mm culture dishes were lysed using 500 μl of lysis buffer (25 mM HEPES [pH 7.4], 150 mM NaCl, 1% NP-40, 1 mM EDTA, 2% glycerol, 1 mM phenylmethylsulfonyl fluoride [PMSF]). After being maintained on ice for 30 min, the lysates were clarified by microcentrifugation at 12,000 rpm for 10 min. To preclear the supernatants, the lysates were incubated with 20 μl of agarose beads (Calbiochem, Cambridge, MA) for 1 h with rotation at 4°C. After centrifugation at 2,000 rpm for 1 min, the supernatants were incubated with 20 μl of antibody-cross-linked protein G-agarose beads overnight at 4°C. Then, the agarose beads were washed six times with wash buffer (25 mM HEPES [pH 7.4], 150 mM NaCl, 0.5% NP-40, 1 mM EDTA, 2% glycerol, 1 mM PMSF). After removing all the liquid, the pelleted beads were resuspended in 30 μl of 1 M glycine (pH 3), after which 10 μl of 4× sampling buffer was added, the samples were denatured, and the sample components were electrophoretically separated on SDS-polyacrylamide gels.

EMSA. Electrophoretic mobility shift assay (EMSA) analyses were performed using a LightShift chemiluminescent EMSA kit obtained from Pierce Biotechnology (Rockford, IL). The following DNA probes containing specific binding sites were used: for c-Jun, sense probe 5′-CGCTTGATGACTCAGC CGG-3′ and antisense probe 5′-CCGGCTGAGTCATCAAGCG-3′, and for OCT-1, sense probe 5′-TGTCGAA TGCAAATCACTAGAA-3′ and antisense probe 5′-TTCTAGTGATTTGCATTCGACA-3′.

Subcutaneous xenografts in nude mice. Female BALB/c nude mice (age, 6 to 7 weeks; weight, 23 to 25 g) were purchased from the Experimental Animal Center of the Guangzhou University of Chinese Medicine (Guangzhou, China) and were randomly divided into four groups ($n = 5$ mice per group). The indicated cells (5×10^6) were suspended in 200 μl of sterile phosphate-buffered saline and were subcutaneously implanted into the flanks of the nude mice. Tumor size was measured with calipers every 6 days, and the volume was calculated as $(\text{width})^2 \times \text{length} \times 0.52$. At day 32 after implantation, all mice were sacrificed, and their tumors were excised. The usage of mice in this work was approved by the Animal Care Committee of Zhongshan School of Medicine, Sun Yat-sen University.

Intracranial brain tumor xenografts and H&E staining. The glioma cells (5×10^5) indicated above were stereotactically implanted into the brains of individual mice ($n = 5$ mice per group). The mice were monitored daily and euthanized when they were moribund. Whole brains were removed, paraffin embedded, sectioned onto 5-μm-thick slides, and hematoxylin and eosin (H&E) stained or immunostained with the following antibodies: anti-CD31 (1:100; catalog number M0823; Dako, Carpinteria, CA) and anti-Ki67 (1:100; catalog number M7240; Dako). Images were captured using an AxioVision (release 4.6) computerized image analysis system (Carl Zeiss, Oberkochen, Germany). The proliferation index was quantified by determining the proportion of Ki67-positive cells by counting. Microvascular density was quantified by counting the CD31-positive cells. The usage of mice in this work was approved by the Animal Care Committee of Zhongshan School of Medicine, Sun Yat-sen University.

IHC. Immunohistochemistry (IHC) analysis of 149 paraffin-embedded, archived samples of glioma specimens was performed. Following deparaffinization, the sections were immunostained using antibodies directed against CD31 (1:100; catalog number M0823; Dako), Ki67 (1:100; catalog number M7240; Dako), VEGF-A (1:200; catalog number ab46154; Abcam), c-MET (1:200; catalog number 3189; Cell Signaling), cyclin D1 (1:200; catalog number ab134175; Abcam), or MMP-2 (1:200; catalog number ab37150; Abcam). The intensity of immunostaining was scored separately by two independent pathologists. The staining index (SI) values were calculated as follows: staining intensity score × proportion of positively stained tumor cells. The staining intensity and proportion of tumor cells positively stained for the proteins indicated above were determined in 10 randomly selected microscopic fields, and we calculated the average SI for the 10 selected fields. Cutoff values for high and low levels of expression of the proteins of interest were chosen to reflect the heterogeneity of the immunostaining results. The chi-square test was used to analyze the relationship between the level of AEG-1 expression and the levels of expression of the other genes. Images of the immunostained sections were captured using an AxioVision (release 4.6) computerized image analysis system (Carl Zeiss).

Microarray data processing and visualization. Microarray hybridization, data generation, and normalization were performed at the Shanghai Biochip Corporation following standard Agilent protocols. Bioinformatics analysis and visualization of the microarray data were performed using MeV (version 4.6) software (http://www.tm4.org/#/welcome).

Gene set enrichment analysis. GSEA was performed using the GSEA (version 2.0.9) platform (http://www.broadinstitute.org/gsea/). The samples were divided into groups with high levels of AEG-1 and groups with low levels of AEG-1 on the basis of the median level of AEG-1 expression. The c-Jun-activated genes included in our analysis were *BDKRB1*, *BTK*, *CCND1*, *CCR7*, *CDH5*, *CHST1*, *DYRK1A*, *EDN1*, *GFAP*, *GLI2*, *HS3ST3B1*, *HSPB7*, *IGSF3*, *IL-9*, *KCNK10*, *LAPTM5*, *LOR*, *MCF2L*, *MET*, *MMP2*, *MMP9*, *MYC*, *PDE4D*, *PLA2G2E*, *PRDM13*, *SERPINE1*, *SOST*, *TFB1M*, and *VEGFA*.

Statistical analysis. All statistical analyses were conducted using the SPSS (version 10.0) statistical software package. The relationship between the level of AEG-1 expression and the levels of expression

of CD31, Ki67, VEGF-A, c-MET, cyclin D1, and MMP-2 determined by immunohistochemistry analysis were analyzed using the chi-square test. Spearman's correlation coefficients were calculated to determine the strength of the relationship between the expression levels of AEG-1 and the transcriptional activity levels of c-Jun. Mean values ± SDs were calculated, and two-tailed Student's *t* tests were performed to compare paired samples using the data analysis tools provided in the software package. In all cases, a *P* value of <0.05 was considered to indicate a significant difference.

Accession number(s). The microarray data described herein have been deposited in the National Center for Biotechnology Information Gene Expression Omnibus database (http://www.ncbi.nlm.nih.gov/geo/) under accession number GSE29952.

SUPPLEMENTAL MATERIAL

Supplemental material for this article may be found at https://doi.org/10.1128/MCB.00456-16.

TEXT S1, PDF file, 0.3 MB.
TEXT S2, PDF file, 0.3 MB.
TEXT S3, XLSX file, 2.0 MB.

ACKNOWLEDGMENTS

This work was supported by the Natural Science Foundation of China (no. 81272339, 81330058, 91529301, and 81325013), Guangdong Natural Science Funds for Distinguished Young Scholars (2014A030306023), the Science and Technology of Guangdong Province (no. 2014A030313008), and the National Science and Technique Major Project (201305017).

We declare no competing financial interests.

REFERENCES

1. Taran SJ, Taran R, Batra M, Ladia DD, Bhandari V. 2015. Survival with concurrent temozolomide and radiotherapy in pediatric brainstem glioma with relation to the tumor volume. J Pediatr Neurosci 10:341–345. https://doi.org/10.4103/1817-1745.174453.
2. VandenDriessche T, Chuah MK. 2013. Glioblastoma: bridging the gap with gene therapy. Lancet Oncol 14:789–790. https://doi.org/10.1016/S1470-2045(13)70342-5.
3. Su ZZ, Kang DC, Chen Y, Pekarskaya O, Chao W, Volsky DJ, Fisher PB. 2003. Identification of gene products suppressed by human immunodeficiency virus type 1 infection or gp120 exposure of primary human astrocytes by rapid subtraction hybridization. J Neurovirol 9:372–389. https://doi.org/10.1080/13550280390201263.
4. Su ZZ, Kang DC, Chen Y, Pekarskaya O, Chao W, Volsky DJ, Fisher PB. 2002. Identification and cloning of human astrocyte genes displaying elevated expression after infection with HIV-1 or exposure to HIV-1 envelope glycoprotein by rapid subtraction hybridization, RaSH. Oncogene 21:3592–3602. https://doi.org/10.1038/sj.onc.1205445.
5. Su ZZ, Chen Y, Kang DC, Chao W, Simm M, Volsky DJ, Fisher PB. 2003. Customized rapid subtraction hybridization (RaSH) gene microarrays identify overlapping expression changes in human fetal astrocytes resulting from human immunodeficiency virus-1 infection or tumor necrosis factor-alpha treatment. Gene 306:67–78. https://doi.org/10.1016/S0378-1119(03)00404-9.
6. Kang DC, Su ZZ, Sarkar D, Emdad L, Volsky DJ, Fisher PB. 2005. Cloning and characterization of HIV-1-inducible astrocyte elevated gene-1, AEG-1. Gene 353:8–15. https://doi.org/10.1016/j.gene.2005.04.006.
7. Emdad L, Sarkar D, Su ZZ, Randolph A, Boukerche H, Valerie K, Fisher PB. 2006. Activation of the nuclear factor kappaB pathway by astrocyte elevated gene-1: implications for tumor progression and metastasis. Cancer Res 66:1509–1516. https://doi.org/10.1158/0008-5472.CAN-05-3029.
8. Sarkar D, Park ES, Emdad L, Lee SG, Su ZZ, Fisher PB. 2008. Molecular basis of nuclear factor-kappaB activation by astrocyte elevated gene-1. Cancer Res 68:1478–1484. https://doi.org/10.1158/0008-5472.CAN-07-6164.
9. Thirkettle HJ, Mills IG, Whitaker HC, Neal DE. 2009. Nuclear LYRIC/AEG-1 interacts with PLZF and relieves PLZF-mediated repression. Oncogene 28:3663–3670. https://doi.org/10.1038/onc.2009.223.
10. Yoo BK, Santhekadur PK, Gredler R, Chen D, Emdad L, Bhutia S, Pannell L, Fisher PB, Sarkar D. 2011. Increased RNA-induced silencing complex (RISC) activity contributes to hepatocellular carcinoma. Hepatology 53:1538–1548. https://doi.org/10.1002/hep.24216.
11. Blanco MA, Aleckovic M, Hua Y, Li T, Wei Y, Xu Z, Cristea IM, Kang Y. 2011. Identification of staphylococcal nuclease domain-containing 1 (SND1) as a Metadherin-interacting protein with metastasis-promoting functions. J Biol Chem 286:19982–19992. https://doi.org/10.1074/jbc.M111.240077.
12. Meng X, Zhu D, Yang S, Wang X, Xiong Z, Zhang Y, Brachova P, Leslie KK. 2012. Cytoplasmic Metadherin (MTDH) provides survival advantage under conditions of stress by acting as RNA-binding protein. J Biol Chem 287:4485–4491. https://doi.org/10.1074/jbc.C111.291518.
13. Yoo BK, Emdad L, Su ZZ, Villanueva A, Chiang DY, Mukhopadhyay ND, Mills AS, Waxman S, Fisher RA, Llovet JM, Fisher PB, Sarkar D. 2009. Astrocyte elevated gene-1 regulates hepatocellular carcinoma development and progression. J Clin Invest 119:465–477. https://doi.org/10.1172/JCI36460.
14. Li G, Wang Z, Ye J, Zhang X, Wu H, Peng J, Song W, Chen C, Cai S, He Y, Xu J. 2014. Uncontrolled inflammation induced by AEG-1 promotes gastric cancer and poor prognosis. Cancer Res 74:5541–5552. https://doi.org/10.1158/0008-5472.CAN-14-0968.
15. Yoo BK, Emdad L, Lee SG, Su ZZ, Santhekadur P, Chen D, Gredler R, Fisher PB, Sarkar D. 2011. Astrocyte elevated gene-1 (AEG-1): a multifunctional regulator of normal and abnormal physiology. Pharmacol Ther 130:1–8. https://doi.org/10.1016/j.pharmthera.2011.01.008.
16. Brown DM, Ruoslahti E. 2004. Metadherin, a cell surface protein in breast tumors that mediates lung metastasis. Cancer Cell 5:365–374. https://doi.org/10.1016/S1535-6108(04)00079-0.
17. Lee SG, Su ZZ, Emdad L, Sarkar D, Fisher PB. 2006. Astrocyte elevated gene-1 (AEG-1) is a target gene of oncogenic Ha-ras requiring phosphatidylinositol 3-kinase and c-Myc. Proc Natl Acad Sci U S A 103:17390–17395. https://doi.org/10.1073/pnas.0608386103.
18. Srivastava J, Siddiq A, Gredler R, Shen XN, Rajasekaran D, Robertson CL, Subler MA, Windle JJ, Dumur CI, Mukhopadhyay ND, Garcia D, Lai Z, Chen Y, Balaji U, Fisher PB, Sarkar D. 2015. Astrocyte elevated gene-1 and c-Myc cooperate to promote hepatocarcinogenesis in mice. Hepatology 61:915–929. https://doi.org/10.1002/hep.27339.
19. Liu L, Wu J, Ying Z, Chen B, Han A, Liang Y, Song L, Yuan J, Li J, Li M. 2010. Astrocyte elevated gene-1 upregulates matrix metalloproteinase-9 and induces human glioma invasion. Cancer Res 70:3750–3759. https://doi.org/10.1158/0008-5472.CAN-09-3838.
20. Wang YN, Chen YJ, Chang WC. 2006. Activation of extracellular signal-regulated kinase signaling by epidermal growth factor mediates c-Jun

activation and p300 recruitment in keratin 16 gene expression. Mol Pharmacol 69:85–98.
21. Chen YJ, Wang YN, Chang WC. 2007. ERK2-mediated C-terminal serine phosphorylation of p300 is vital to the regulation of epidermal growth factor-induced keratin 16 gene expression. J Biol Chem 282:27215–27228. https://doi.org/10.1074/jbc.M700264200.
22. Vries RG, Prudenziati M, Zwartjes C, Verlaan M, Kalkhoven E, Zantema A. 2001. A specific lysine in c-Jun is required for transcriptional repression by E1A and is acetylated by p300. EMBO J 20:6095–6103. https://doi.org/10.1093/emboj/20.21.6095.
23. Chang HJ, Park JS, Kim MH, Hong MH, Kim KM, Kim SM, Shin BA, Ahn BW, Jung YD. 2006. Extracellular signal-regulated kinases and AP-1 mediate the up-regulation of vascular endothelial growth factor by PDGF in human vascular smooth muscle cells. Int J Oncol 28:135–141.
24. Damert A, Ikeda E, Risau W. 1997. Activator-protein-1 binding potentiates the hypoxia-inducible factor-1-mediated hypoxia-induced transcriptional activation of vascular-endothelial growth factor expression in C6 glioma cells. Biochem J 327(Pt 2):419–423.
25. Cho ML, Jung YO, Moon YM, Min SY, Yoon CH, Lee SH, Park SH, Cho CS, Jue DM, Kim HY. 2006. Interleukin-18 induces the production of vascular endothelial growth factor (VEGF) in rheumatoid arthritis synovial fibroblasts via AP-1-dependent pathways. Immunol Lett 103:159–166. https://doi.org/10.1016/j.imlet.2005.10.020.
26. Mathas S, Hinz M, Anagnostopoulos I, Krappmann D, Lietz A, Jundt F, Bommert K, Mechta-Grigoriou F, Stein H, Dorken B, Scheidereit C. 2002. Aberrantly expressed c-Jun and JunB are a hallmark of Hodgkin lymphoma cells, stimulate proliferation and synergize with NF-kappa B. EMBO J 21:4104–4113. https://doi.org/10.1093/emboj/cdf389.
27. Assimakopoulou M, Kondyli M, Gatzounis G, Maraziotis T, Varakis J. 2007. Neurotrophin receptors expression and JNK pathway activation in human astrocytomas. BMC Cancer 7:202. https://doi.org/10.1186/1471-2407-7-202.
28. Lopez-Bergami P, Lau E, Ronai Z. 2010. Emerging roles of ATF2 and the dynamic AP1 network in cancer. Nat Rev Cancer 10:65–76. https://doi.org/10.1038/nrc2681.
29. Cui J, Wang Q, Wang J, Lv M, Zhu N, Li Y, Feng J, Shen B, Zhang J. 2009. Basal c-Jun NH_2-terminal protein kinase activity is essential for survival and proliferation of T-cell acute lymphoblastic leukemia cells. Mol Cancer Ther 8:3214–3222. https://doi.org/10.1158/1535-7163.MCT-09-0408.
30. Cui J, Han SY, Wang C, Su W, Harshyne L, Holgado-Madruga M, Wong AJ. 2006. c-Jun NH(2)-terminal kinase 2alpha2 promotes the tumorigenicity of human glioblastoma cells. Cancer Res 66:10024–10031. https://doi.org/10.1158/0008-5472.CAN-06-0136.
31. Tsuiki H, Tnani M, Okamoto I, Kenyon LC, Emlet DR, Holgado-Madruga M, Lanham IS, Joynes CJ, Vo KT, Wong AJ. 2003. Constitutively active forms of c-Jun NH_2-terminal kinase are expressed in primary glial tumors. Cancer Res 63:250–255.
32. Uchida C, Gee E, Ispanovic E, Haas TL. 2008. JNK as a positive regulator of angiogenic potential in endothelial cells. Cell Biol Int 32:769–776. https://doi.org/10.1016/j.cellbi.2008.03.005.
33. Debinski W, Gibo D, Mintz A. 2003. Epigenetics in high-grade astrocytomas: opportunities for prevention and detection of brain tumors. Ann N Y Acad Sci 983:232–242. https://doi.org/10.1111/j.1749-6632.2003.tb05978.x.
34. Eferl R, Wagner EF. 2003. AP-1: a double-edged sword in tumorigenesis. Nat Rev Cancer 3:859–868. https://doi.org/10.1038/nrc1209.
35. Wagner EF, Nebreda AR. 2009. Signal integration by JNK and p38 MAPK pathways in cancer development. Nat Rev Cancer 9:537–549. https://doi.org/10.1038/nrc2694.
36. Vivanco I, Palaskas N, Tran C, Finn SP, Getz G, Kennedy NJ, Jiao J, Rose J, Xie W, Loda M, Golub T, Mellinghoff IK, Davis RJ, Wu H, Sawyers CL. 2007. Identification of the JNK signaling pathway as a functional target of the tumor suppressor PTEN. Cancer Cell 11:555–569. https://doi.org/10.1016/j.ccr.2007.04.021.
37. Lamph WW, Wamsley P, Sassone-Corsi P, Verma IM. 1988. Induction of proto-oncogene JUN/AP-1 by serum and TPA. Nature 334:629–631. https://doi.org/10.1038/334629a0.
38. Herdegen T, Waetzig V. 2001. AP-1 proteins in the adult brain: facts and fiction about effectors of neuroprotection and neurodegeneration. Oncogene 20:2424–2437. https://doi.org/10.1038/sj.onc.1204387.
39. Li J, Zhang N, Song LB, Liao WT, Jiang LL, Gong LY, Wu J, Yuan J, Zhang HZ, Zeng MS, Li M. 2008. Astrocyte elevated gene-1 is a novel prognostic marker for breast cancer progression and overall patient survival. Clin Cancer Res 14:3319–3326. https://doi.org/10.1158/1078-0432.CCR-07-4054.